Eur. Phys. J. A **19**, 341–345 (2004)
DOI 10.1140/epja/i2003-10138-7

THE EUROPEAN PHYSICAL JOURNAL A

Proton- and neutron-induced fission on uranium carbide target

A. Andrighetto[2], A.E. Barzakh[1], D.V. Fedorov[1], V.S. Ivanov[1], G. Lhersonneau[2], F.V. Moroz[1], S.Yu. Orlov[1], V.N. Panteleev[1], M.D. Seliverstov[1], I.M. Strachnov[1], L. Stroe[2], L.B. Tecchio[2,a], Yu.M. Volkov[1], and X.F. Wang[2]

[1] Petersburg Nuclear Physics Institute, 188350, Gatchina, Russia
[2] Laboratori Nazionali di Legnaro, Viale dell'Università 2, 35020 Legnaro (Padova), Italy

Received: 3 July 2003 / Revised version: 2 October 2003 /
Published online: 27 January 2004 –
Communicated by C. Signorini

Abstract. In the frame of the R&D program for the SPES project of the Legnaro Laboratories, the production yields of Rb, In and Cs isotopes have bean measured at the synchrocyclotron of the Petersburg Nuclear Physics Institute (PNPI) of Gatchina (Russia). Production yields for direct proton fission and neutron-induced fission on a high-density UC_2 powder target are compared. The overall efficiencies as a function of the target temperature have been measured.

PACS. 24.75.+i General properties of fission – 25.85.Ec Neutron-induced fission

Introduction

The possibility to produce intense beams of accelerated radioactive ions of unstable nuclei has been worldwide recognized by the scientific community as a new horizon for nuclear physics and many other disciplines making use of nuclear probes. A fast look at the nuclide chart immediately shows the vast unknown territories on the neutron-rich side of the valley of β-stability, which are the most interesting for nuclear physics. The SPES (Study and Production of Exotic Species) project [1] of the Legnaro National Laboratories (LNL), based on the availability of the post accelerator ALPI [2], is conceived for delivering intense, high-quality beams of short-lived neutron-rich nuclei, at energies of about 20 MeV per nucleon, in the mass region 80–160 a.m.u.

A flux of fast neutrons generated by the interaction of 1 mA–100 MeV proton beam in a thick target (neutron converter) of sufficient thickness to stop all the protons and other charged particles produced by the reactions will induce fission of natural uranium (uranium carbide) target placed downstream of the converter, with the aim of 10^{13} fissions/s at least. With the use of neutron-induced fission of ^{238}U, a wide distribution extending to very neutron-rich isotopes is obtained mainly by neutrons in the low-energy part of the spectrum. This production scheme was introduced by the Argonne Laboratory [3] to remove from the fissile target the heat produced by the slowing-down of the charged beam, mostly due to electronic stopping, whereas the useful nuclear reaction (*i.e.* fission) takes place in the fission target. First experimental results have been reported in ref. [4].

In the frame of the R&D program for the SPES project we have measured the production yields of the isotopes of Rb, In and Cs, comparing the production yields for direct proton fission and neutron-induced fission on the same UC_2 target. The production yields as a function of the target temperature, as well as the diffusion times for the nuclei mentioned above, have been measured.

Experimental techniques

The measurements have been performed at the IRIS ISOL-system [5] at the synchrocyclotron of the Petersburg Nuclear Physics Institute (PNPI) of Gatchina (Russia) with a proton beam of energy 1 GeV and current 0.05 μA. The beam is transported over a distance of 60 m to the target area. There, it impinges directly on the UC_2 target or is deflected by a magnet to impinge on a tantalum converter to generate fast neutrons. A sketch of the target set-up is depicted in fig. 1. The products of proton/neutron beam interaction with the UC target after ionization and acceleration (30 kV) are selected by a magnet located in the shielding wall. Then, the ion beam is implanted into a moving collector tape and the radioactivity is detected by a γ-detector. The transmission of the beamline used for the yield measurement was 3%.

A schematic view of the target/ion source assembly is shown in fig. 2. One of the essential issues of the target construction is the use of a tungsten container in which the graphite container, with the target material, is housed.

[a] e-mail: tecchio@lnl.infn.it

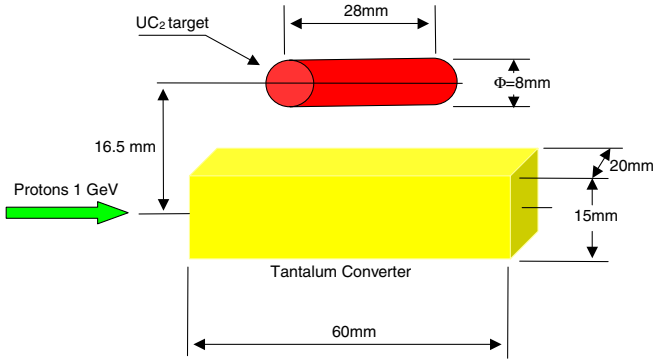

Fig. 1. Sketch of the experimental target set-up. The proton beam can be switched to impinge directly on the UC target or on the tantalum converter.

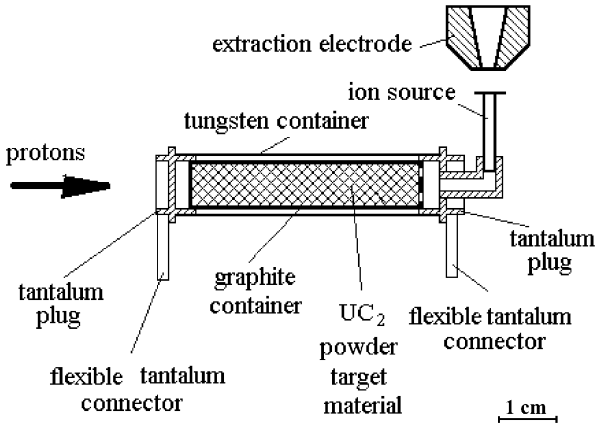

Fig. 2. Schematic view of the target/ion source assembly.

The employment of the most temperature-resistant material, such as tungsten with melting point at 3422 °C, allows to keep the target temperature as high as needed to ensure a fast release of the reaction products from the target material and from the target container volume [6]. The graphite container preserves the tungsten container from the very aggressive chemical corrosion of uranium. Both target and ion source were operated in the temperature interval of (2100–2400) °C by Ohmic heating, independently.

The target material consists of High Density Powder (HDP) uranium carbide, obtained from the fragmentation of High Density Rod (HDR) uranium carbide (UC_2) of density 11.2 gcm^{-3}. The HDP target has a volume of 1.4 cm^3 (ϕ = 8 mm, L = 28 mm) and contains about 10 grams of uranium with an effective density of 7.36 gcm^{-3} (corresponding to a target thickness of about 20 gcm^{-2}). The average grain size was about 10–20 μm.

To ensure good working conditions of the ion source, it is important to keep the pressure below 10^{-4} Torr. This requires high purity of the materials used in the entire assembly. Furthermore, an outgassing procedure which lasts for more than 72 h at temperatures of 1800–2300 °C is necessary. This is normally done at an off-line target pump stand, which is identical to those of the on-line separator. Temperature calibration of the target container and ion source as a function of the applied current is performed

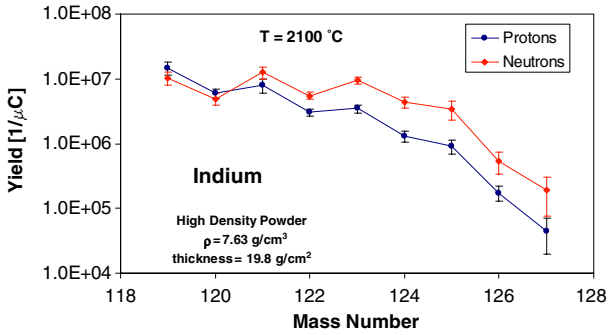

Fig. 3. Yields of neutron-rich In isotopes. Comparison between the production rates for proton- and neutron-induced fission. The production rates for neutron-induced fission are corrected for the total neutron flux generated in the whole solid angle. The solid lines are only to guide the eye.

with an optical pyrometer through a glass window in the vacuum chamber.

Typical surface-ionization ion sources made in tungsten were employed. To test the ion source operation, an off-line mass separator system has been used. At 2100 °C ionization efficiencies of 30–35% for Rb and Cs and 1–3% for In have been measured using the well-knwon implantation technique [7]. The work function ϕ of a pure tungsten surface sharply decreases at a temperature of 2300–2400 °C ($\phi < 4.5$ eV) due to the interaction of carbon vapor with the surface and subsequent formation of a thermally very stable carbide of tungsten. These circumstances lead to a decrease of the ionization efficiency for elements with ionization potentials higher than 4.5 eV.

The identification of the mass-separated nuclides was performed using a tape transport system, working in the "start-stop" regime and transporting the activity to a γ-radiation detector. The latter was a Ge(Li) (160 cm^3) detector of 1.2% total peak efficiency at 1.3 MeV placed at about 1.5 cm from the tape. The energy range covered was from 100 keV to 2 MeV. The delay curves were obtained by sampling the radioactive beam at rectangular regular intervals after switching off the proton beam and bringing the sources one by one in front of the γ-detector.

Results and discussion

The observed yields of neutron-rich Rb, In and Cs isotopes, given as ion per μC determined at the exit of the ion source, are summarized in figs. 3–5. The figures show the comparison of the production yields for direct fission induced by the proton beam on the target and for fission induced by neutrons generated in a tantalum block on the same UC_2 target, as depicted in fig. 1. The error bars take into account common systematic errors connected to the experimental set-up and specific errors on the γ-counting. Both the UC_2 target and the ion source during the measurements were operated at the same temperature of 2100 °C. The MCNPx Monte Carlo code [8] showed that the neutron production rate from the tantalum block is 5.1 n/p and that only 4% of them are impinging into

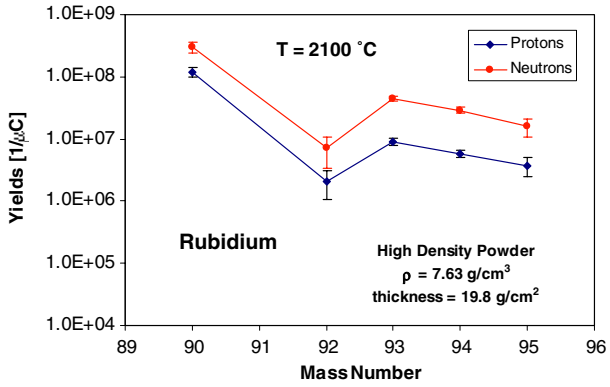

Fig. 4. Yields of neutron-rich Rb isotopes. Comparison between the production rates for proton- and neutron-induced fission, as above. The discontinuity for ^{92}Rb with respect to the trend of the curve is discussed in the text.

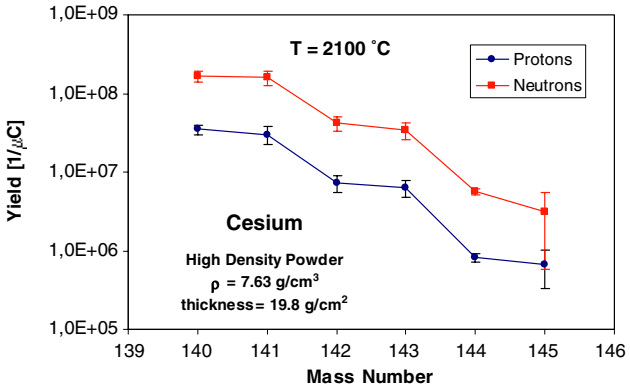

Fig. 5. Yields of neutron-rich Cs isotopes. Comparison between the production rates for proton- and neutron-induced fission, as above.

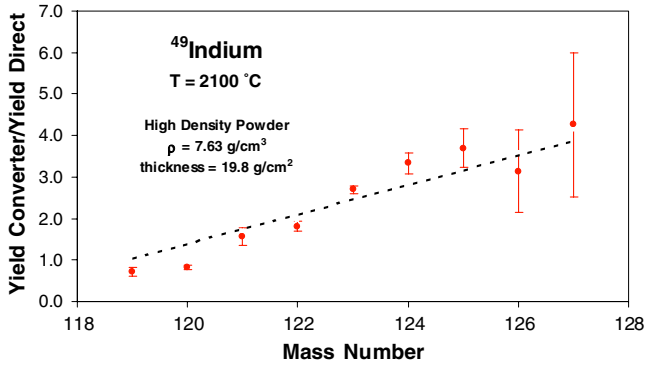

Fig. 6. Yield ratios between neutron- and proton-induced fission, for indium isotopes, at the target temperature of 2100 °C. The dots show the experimental values and the dashed curve represents the general trend of the data reproduced as reported in ref. [10], with a shift of the centre of the distributions $\Delta Z = 0.2$ and a renormalization factor of 3.

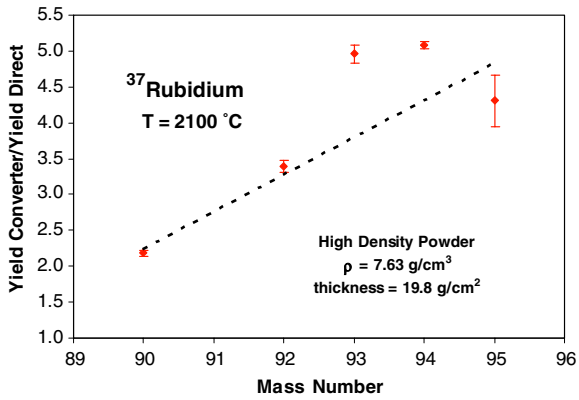

Fig. 7. Yield ratios between neutron- and proton-induced fission, for rubidium isotopes, as above. The renormalization factor is 3.2.

the uranium carbide target. Hence, the production yields generated by neutrons are corrected supposing the neutrons produced in the whole solid angle impinging into the target, to better compare with the yields from proton-induced fission. In the case of fission induced by neutrons, the production of neutron-rich isotopes is enhanced for nuclei far from the β-stability, being a probable consequence of the lower average excitation energy and of larger N/Z of the fissioning nucleus. Because of the low gamma branching ratio in the energy range covered by the detector, the isotope ^{91}Rb was not detected. The discontinuity for ^{92}Rb in both curves is probably due to the spectroscopic input data. The Nuclear Data Sheets [9] list very different absolute gamma intensities per decay reported by various groups. The oldest value (with a ground-state (g.s.) branching of 94%) indeed removes the discontinuity but renders the log ft value for the g.s. branch too low. A yet not discovered isomer could be tentatively invoked as the reason for these inconsistencies.

All the isotopic distributions show a significant odd-even structure, with the formation of even neutron isotopes being favoured. This effect varies more or less smoothly with mass number, but shows no apparent dependence on the production method.

Figures 6–8 show the ratios of the production yields with converter from the direct fission induced by protons. These figures clearly indicate that n-induced fission moves the distribution of isotopes towards the neutron-rich side with respect to p-induced fission. The dashed line in figs. 6, 7 and 8 represent a general trend calculated under the assumption that for a series of isobars the Z-dependence of cross-sections is Gaussian. According to ref. [10], the width and the centre of the distributions of the cross-sections for 25 MeV protons and neutron spectra of about 20 MeV average energy are both well described with a constant and a linear relationship function of the mass number. The ratio of cross-sections $\sigma_{\rm n}(Z,A)/\sigma_{\rm p}(Z,A)$ in the present experiment is reproduced with a FWHM = 1.65 from ref. [10] and by shifting the centre of the distributions by $\Delta Z = 0.2$ (to lower Z values for neutron-induced fission, resulting in about one additional mass unit for a certain element). In addition, a slight renormalisation of the overall scales varying between 3 and 5 for the elements studied here has been applied for better agreement. It suggests that

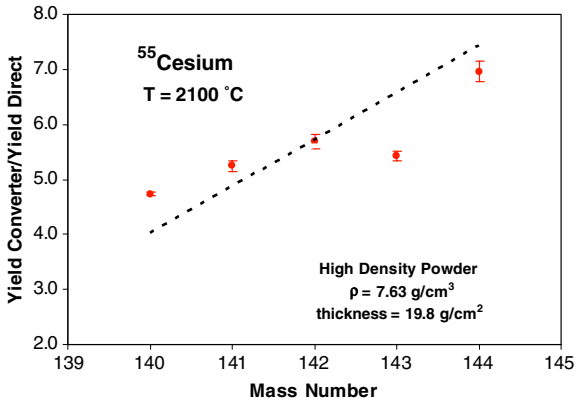

Fig. 8. Yield ratios between neutron- and proton-induced fission, for cesium isotopes, as above. The renormalization factor is 5.0.

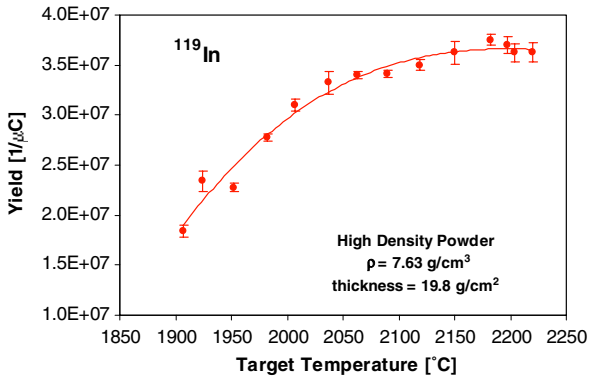

Fig. 9. Production intensity in function of temperature, for ^{119}In. The yields are produced by direct fission induced by protons on the target. At about 2100 °C, the saturation indicates the diffusion-effusion to reach its maximum. The error bars reproduce statistical errors; the systematic error is 13%. The solid line is only to guide the eye and give the trend of data.

cross-sections for n + U could be larger than for p + U. However, a reasonable agreement is also achieved increasing both the width of the distribution and shift ΔZ. Consequently, while the general trend is understood, it is premature to make a strong statement about the details of the distributions.

The production intensities were measured as a function of temperature by monitoring specific γ-ray activities. The results are shown in figs. 9–11. As expected, in all cases the intensities increase with temperature. The increase in ionization efficiency in this temperature region may be considered negligible in all cases. The rate of increase reflects mainly the decrease of the hold-up time. It is to notice that indium yields saturate at lower temperature (fig. 9) because the diffusion rate of indium nuclei from the UC_2 target reach its maximum already around 2100 °C. The overall efficiency for In has been estimated from the saturation values to be 1.5% (fig. 9). Under these conditions, the diffusion-effusion efficiency is by definition equal to 1. In this sense, the measured efficiency repre-

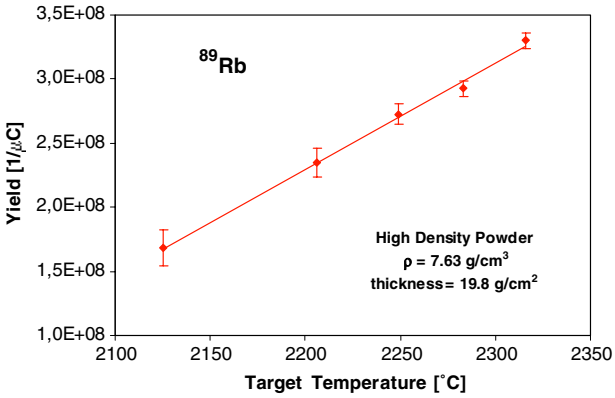

Fig. 10. Production intensity in function of temperature, for ^{89}Rb (as above). No saturation is yet visible unlike in fig. 9. The systematic error is 17%.

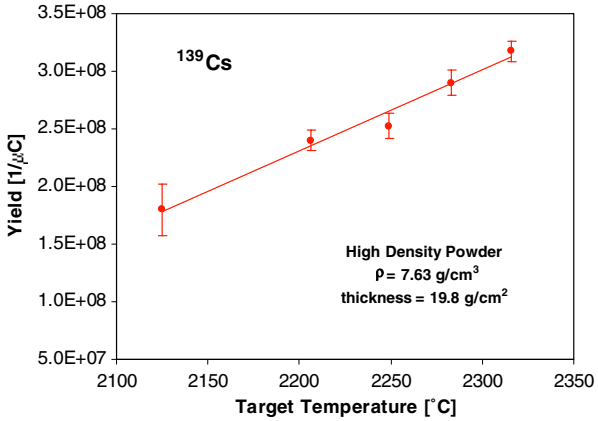

Fig. 11. Production intensity in function of temperature, for ^{139}Cs (as above). The systematic error is 41%.

sents the ionization efficiency which is in good agreement with the off-line measurements.

The main processes whereby radioactive species are lost between initial formation and measurement are associated with diffusion, adsorption, and ion source efficiencies (overall efficiency) for forming beams of the species. The delay time between production and removal of the ionized fission products from the source becomes shorter when increasing the temperature of the target, with the consequent increase of the total efficiency. In fact the release properties of the target are well determined by measuring the overall absolute efficiency [11]. The measured overall efficiencies are shown for ^{89}Rb and ^{139}Cs in fig. 12. These latter were selected because it is seen that nuclides having half-lives around a few minutes or longer are not affected much by the decay losses during the transport process. An efficiency increase of about a factor 2 has been measured in the range of temperatures investigated.

Conclusions

The present experiments clearly show that by using the neutron-induced fission of ^{238}U, a wide mass distribution

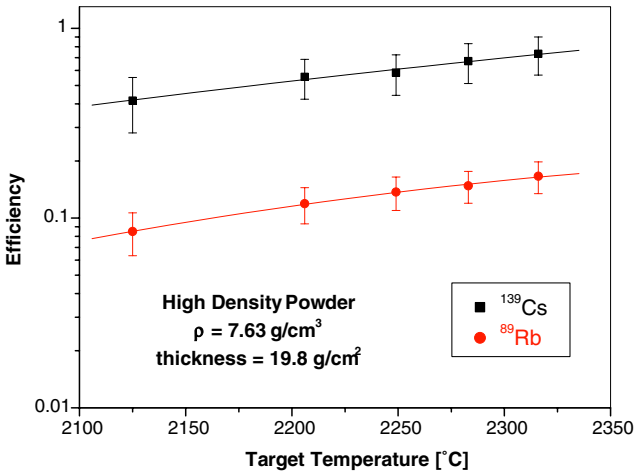

Fig. 12. Overall efficiency as a function of the target temperature for ^{89}Rb ($T_{1/2}$ = 15.2 min) and ^{139}Cs ($T_{1/2}$ = 9.3 min) released from a UC_2 high-density powder target.

extending to very neutron-rich isotopes is obtained. Production yields are enhanced for the neutron-induced fission with respect to the proton-induced fission, mainly for nuclei far from the β-stability.

The overall efficiencies have been estimated using the MCNPx Monte Carlo code [7] giving the in-target production yields at the saturation regime. The increase of the ionization efficiency in the source will lead surely to a proportional increase of the overall efficiency.

Being the in-grain diffusion and the desorption from the surface of the grains the main processes governing the release (delay time) of nuclear-reaction products, it is important for the target development work to investigate which of these processes is the main source of delay.

References

1. A. Bracco, A. Pisent, *SPES - Technical Design for an Advanced Exotic Ion Beam Facility at LNL*, LNL-INFN (REP) 181/02 (2002).
2. A. Dainelli *et al.*, Nucl. Instrum. Methods Phys. Res. A **382**, 100 (1996).
3. J. Nolen, *Proceedings of the Third International Conference on Radioactive Nuclear Beams, East Lansing, Michigan, USA, May 24-27, 1993*, edited by D.J. Morrisey (Editions Frontières, Gif-sur-Yvette, 1993) p. 111.
4. M. Portillo *et al.*, Nucl. Instrum. Methods Phys. Res. B **194**, 193 (2002).
5. V.A. Bolshakov *et al.*, Nucl. Instrum. Methods Phys. Res. B **70**, 69 (1992).
6. V.N. Panteleev, A.E. Barzakh, D.V. Fedorov, F.V. Moroz, A.G. Polyakov, S.Yu. Orlov, M.D. Seliverstov, Yu.M. Volkov, Hyperfine Interact. **127**, 421 (2000).
7. G.D. Alton *et al.*, Nucl. Instrum. Methods Phys. Res. B **66**, 492 (1992).
8. Laurie S. Waters (Editor), MCNPx User Manual, Version 2.1.5, TPO-E83-G-UG-X-00001, November 14, 1999.
9. C.M. Baglin, Nucl. Data Sheets **91**, 423 (2000).
10. G. Lhersonneau *et al.*, Eur. Phys. J. A **9**, 385 (2000); L. Stroe *et al.*, Eur. Phys. J. A **17**, 57 (2003).
11. N. Lecesne *et al.*, Nucl. Instrum. Methods Phys. Res. B **126**, 141 (1997).